Observation of Bridged–Terminal Hydrido Equilibria in a Series of Iron–Platinum Bimetallic Complexes

John Powell,* Michael R. Gregg, and Jeffery F. Sawyer

Department of Chemistry, University of Toronto, Toronto, Ontario, Canada M5S 1A1

Oxidative addition of $Fe(CO)_4PR_2H$ to $Pt(C_2H_4)(PR'_3)_2$ gives an equilibrium mixture of $(OC)_3Fe(\mu\text{-}PR_2)(\mu\text{-}H)Pt(PR'_3)_2$ and $(OC)_3(H)Fe(\mu\text{-}PR_2)Pt(PR'_3)_2$, the first system in which an equilibration between bridge and terminal hydride bonding modes can be observed.

Whilst a large number of transition metal bimetallic and cluster hydrides containing bridging and/or terminal hydrido ligands are known[1] the simple observation of an equilibration between bridge hydrido and terminal hydrido co-ordination modes has not as yet been reported.[2] We here describe a series of heterobimetallic hydrido carbonyl Fe–Pt dimers, the first system in which such an equilibration can be observed.

Oxidative addition of the P–H bond in $Fe(CO)_4PR_2H$ (**1**),[3] [R = Pr^n, Ph, cyclohexyl (Cy)], to zero valent platinum phosphine complexes[4] provides a simple route to complexes of the type $(OC)_3Fe(H)(PR_2)Pt(PR'_3)_2$ [(**2a**) was obtained from the reaction of $(OC)_4FePCy_2Li$ and *trans*-$PtHCl(PEt_3)_2$]. In solution these Fe–Pt dimers equilibrate between a bridged hydride structure (**2a**—**d**), and a terminal hydride form, (**3b**—**e**), as shown in equation (1). The molecular structures of

$Fe(CO)_4PR_2H$

(**1**)

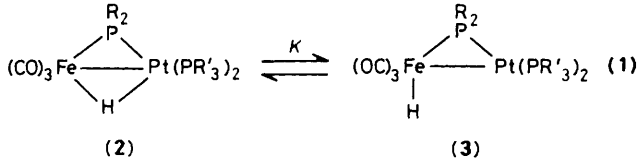

(**1**)

(**2**) (**3**)

the bridged hydrido complex (**2a**), (Figure 1), and the terminal hydrido complex (**3c**) (Figure 2) have been determined by single crystal *X*-ray diffraction.† Although the position of the

† *Crystal data:* (**2a**), crystal quality poor, $C_{27}H_{53}FeP_3PtO_3$, M = 769.6, monoclinic, space group $P2_1/c$, a = 10.010(8), b = 24.695(13), c = 14.152(12) Å, β = 108.50(7)°, U = 3317 Å^3, D_c = 1.54 g cm^{-3} for Z = 4, Mo-$K_{\bar{\alpha}}$ radiation (λ = 0.71069 Å), T = 298 K, μ(Mo-$K_{\bar{\alpha}}$) = 48.6 cm^{-1}. Cell parameters determined using 22 reflections ($6.2 < \theta < 14.1°$). Data collection (Enraf-Nonius CAD4 diffractometer) ω–2θ scans, $(0.85 + 0.35 \tan\theta)°$ scan ranges, max. scan time = 45 s, max. 2θ = 44°, quadrants h, k, $\pm l$ gave 4534 data. Three standards collected every 8500 s showed *ca.* 33% loss in intensities. Lorentz, polarization, crystal decay, and absorption corrections to all data.

(**3c**), $C_{51}H_{41}FeP_3PtO_3$, M = 1045.7, monoclinic, space group $P2_1/c$, a = 10.551(2), b = 19.049(3), c = 24.092(4) Å, β = 98.29(1)°, U = 4792 Å^3, D_c = 1.45 g cm^{-3} for Z = 4, Mo-$K_{\bar{\alpha}}$ radiation (λ = 0.71069 Å), T = 298 K, μ(Mo-$K_{\bar{\alpha}}$) = 33.9 cm^{-1}. Cell parameters determined using 25 reflections ($12.6 < \theta < 17.4°$). Data collection: ω–2θ scans, $(0.70 + 0.35 \tan\theta)°$ scan ranges, max. scan time = 55 s, max. 2θ = 50°, quadrants h, k, $\pm l$ gave 10550 data. Three standards collected every 8500 s showed 35% loss in intensities. Lorentz, polarization, and corrections for crystal decay. Both structures solved by the Patterson method and refined by least-squares to final agreement indices R = 0.1029 (R_w = 0.1224) (**2a**) and R = 0.524 (R_w = 0.0658) (**3c**) using 2189 (**2a**) and 4074 (**3c**) observed [$I > 3\sigma(I)$] data respectively. Weights given by $4F^2\{\sigma^2(I) + (pF^2)^2\}^{-1}$ with p = 0.15 (**2a**) or p = 0.065 (**3c**). Atomic co-ordinates, bond lengths and angles, and thermal parameters have been deposited at the Cambridge Crystallographic Data Centre. See Notice to Authors, Issue No. 1.

Table 1. Spectroscopic and thermodynamic data (CH_2Cl_2 or CD_2Cl_2, 22 °C).

	R	R'	ν(CO)/cm^{-1}	J(Pt–H)/Hz	K	ΔH/ kcal mol^{-1}	ΔS/ cal deg^{-1} mol^{-1}	ΔG/ kcal mol^{-1} [a]
(**2a**)	Cy	Et	1945s, 1863m, 1852m	520	—	—	—	—
(**2b**) (**3b**)	Pr	Ph	1961s, 1885m, 1859m 1999s, 1936m, 1922m	417	0.34	2.16	5.22	0.62
(**2c**) (**3c**)	Ph	Ph	1966s, 1895m, 1873m 2006s, 1947m, 1928m	256	1.16	1.29	4.71	−0.1
(**2d**) (**3d**)	Cy	Ph	1961s, 1883m, 1859m 1998s, 1934m, 1922m	210	2.67	0.095	2.28	−0.58
(**3e**)	Ph	OPh	2020s, 1961m, 1943m	28	—	—	—	—

[a] 1 kcal = 4.184 kJ.

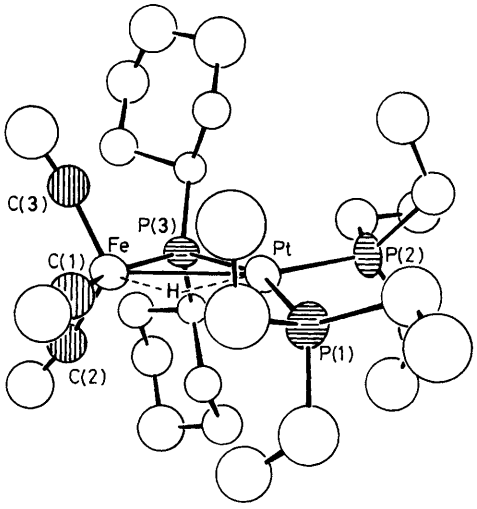

Figure 1. Molecular structure of (**2a**) as determined by single crystal *X*-ray diffraction. Selected bond lengths (Å): Pt–Fe, 2.800(4); Pt–P(1), 2.321(7); Pt–P(2), 2.295(7); Pt–P(3), 2.311(7); Fe–P(3), 2.203(8). Selected bond angles (°): Fe–Pt–P(1), 107.0; Fe–Pt–P(2), 153.2; Fe–Pt–P(3), 49.9; Pt–Fe–P(3), 53.4; Pt–Fe–C(1), 110; Pt–Fe–C(2), 116; Pt–Fe–C(3), 118; C(1)–Fe–C(2), 91; C(1)–Fe–C(3), 93; C(2)–Fe–C(3), 121. The position of the hydride ligand (not determined) is assumed to be bridging Fe–Pt and approximately *trans* to P(2).

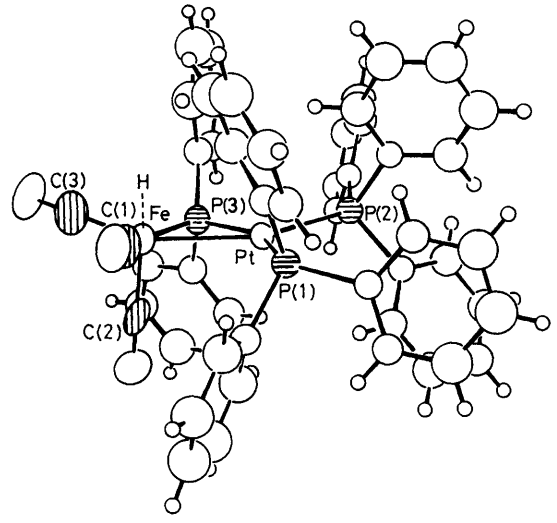

Figure 2. Molecular structure of (**3c**) as determined by single crystal *X*-ray diffraction. Selected bond lengths (Å): Pt–Fe, 2.698(2); Pt–P(1), 2.323(3); Pt–P(2), 2.269(3); Pt–P(3), 2.247(3); Fe–P(3), 2.167(4). Selected bond angles (°): Fe–Pt–P(1), 99.3; Fe–Pt–P(2), 155.6; Fe–Pt–P(3), 51.0; Pt–Fe–P(3), 53.7; Pt–Fe–C(1), 100; Pt–Fe–C(2), 94.9; Pt–Fe–C(3), 150.9; C(1)–Fe–C(2), 97.4; C(1)–Fe–C(3), 101.6; C(2)–Fe–C(3), 101.3. The position of the hydride ligand (not determined) is assumed to be approximately *trans* to C(2).

hydride ligand was not determined in either structure, the location of the hydride ligand as shown in Figures 1 and 2 may be inferred from (i) the disposition of the other ligands; (ii) the similarity of the solid and solution i.r. spectra [ν(CO) region] (Table 1); and (iii) the solution ^{1}H n.m.r. data for the hydride ligand (Table 1 and footnote‡). J(^{195}Pt–^{1}H) data are particularly diagnostic[5] being *ca.* 520 Hz for bridging hydride [*e.g.* (**2a**)] and *ca.* 28 Hz for the terminal (Fe) hydrido isomer [*e.g.* (**3e**)]. Complexes in which both terminal and bridged isomers are present in solution exhibit ν(CO) signals attributable to both isomers and values of J(^{195}Pt–^{1}H) (fast exchange limit) in between those of (**2a**) and (**3e**) (Table 1). On going from the bridged hydrido structure [(**2a**), Figure 1] to the terminal hydrido structure, [(**3c**), Figure 2] the major changes are (i) the disposition of the hydride ligand: approximately perpendicular to the $FePtP_3$ plane in (**3c**) as opposed to in the plane in (**2a**); (ii) the Fe–Pt bond length is *ca.* 0.10 Å shorter in (**3c**); and (iii) the geometry about the Fe in (**3c**) is pseudo octahedral as opposed to pseudo trigonal bipyramidal in (**2a**) [*e.g.* ∠ C(2)–Fe–C(3) is 101(1)° in (**3c**) and 121(1)° in (**2a**) and ∠ Pt–Fe–C(3) is 118(1)° in (**2a**) and 151(1)° in (**3c**)]. The observed distortions from a regular geometry about Fe in both (**2a**) and (**3c**) are consistent with those observed in other hydride systems.[6]

‡ *Selected spectroscopic data:* ^{1}H and ^{31}P n.m.r. (p.p.m. relative to 85% H_3PO_4) δ (CD_2Cl_2), J in Hz. (**2a**): hydrido region: δ (H) 12.25 [Fe(μ-H)Pt, 1:4:1, t of dd, J(P*trans*H) 78, J(P*cis*H) 18, 32, J(^{195}Pt–H) 520]; ^{31}P{^{1}H}: δ 223 [μ-phosphido, 1:4:1, t of dd, J(^{31}P–^{31}P) 205, 12, J(^{195}Pt–^{31}P) 1811], 12 [P*trans*H, 1:4:1, t of dd, J(^{31}P–^{31}P) 12, 18, J(^{195}Pt–^{31}P) 3585], 12 [P*cis*H, 1:4:1, t of dd, J(^{31}P–^{31}P) 18, 205, J(^{195}Pt–^{31}P) 2342]. (**3e**): hydrido region: δ(H) 12.03 [Fe–H, 1:4:1, t of ddd, J(μ-phosphido-H) 57, J(^{31}P–H) 8.8, 5.8, J(^{195}Pt–H) 28]; ^{31}P{^{1}H}: δ 172 [μ-phosphido, 1:4:1, t of dd, J(^{31}P^{31}P) 28, 328, J(^{195}Pt–^{31}P) 2326], 137 [P*trans*-μ-phosphido, 1:4:1, t of dd, J(^{31}P–^{31}P) 4328, J(^{195}Pt–^{31}P) 5152], 124 [P*cis*-μ-phosphido, 1:4:1, t of dd, J(^{31}P–^{31}P) 4, 28, J(^{195}Pt–^{31}P) 5514].

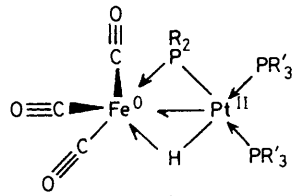

(I)

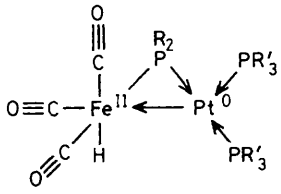

(II)

The observed co-ordination geometry at Fe (Figure 1) and ν(CO) data for the bridged hydrido isomer (**2**) (Table 1) are reasonably consistent with the $Pt^{II}Fe^{0}$ structural representation (I). The observed bridged hydrido–terminal hydrido equilibration [equation (1)] may be regarded as an intramolecular redox isomerism with the terminal hydrido structure (**3**) having a more oxidized Fe and reduced Pt as indicated by the representation (II). Oxidation of Fe is indicated by the observed blue shift of ν(CO) of (**3**) (50—100 cm^{-1}) and the pseudo octahedral co-ordination of Fe in (**3**) (Figure 2). As might be expected the relative amount of the terminal hydride (**3**) and the extent of Fe oxidation [ν(CO) blue shift of (**3**) relative to (**2**)] are very sensitive to the nature of the ligands bonded to Pt. A ligand capable of stabilizing Pt in a low oxidation state [*e.g.* $P(OPh)_3$, complex (**3e**)] results in only the terminal hydride being observed and a blue shift of ν(CO) of *ca.* 100 cm^{-1} relative to (**2a**) is not inconsistent with the $Fe^{II}Pt^{0}$ representation (II), whilst for the good donor phosphine PEt_3 only the bridged hydrido $Fe^{0}Pt^{II}$ complex (**2a**) is observed.

For the systems where both bridged and terminal hydrido forms are readily observed {(**2b**—**d**) ⇌ (**3b**—**d**)} the rate of (**2**) ⇌ (**3**) interchange is still rapid on the ^1H n.m.r. time scale at −90 °C [estimated E_a for bridge ⇄ terminal exchange ≤6 kcal/mol; 1 kcal = 4.184 kJ]. Using the observed $J(^{195}Pt–^1H)$ values of the totally bridged (**2a**) and the totally terminal (**3e**) as typical of the two structural forms the observed average $J(^{195}Pt–^1H)$ (hydride) for the systems (**2b**—**d**) ⇌ (**3b**—**d**) can be utilized to determine the equilibrium constant [equation (1)] at a particular temperature. Values of K (22 °C) and thermodynamic data are given in Table 1. For the systems where both isomers are observable, the terminal hydrido isomer (**3b**—**d**) is the favoured high temperature form. The enthalpy difference between the two isomeric forms is very small. The data suggest that the bridge–terminal hydrido rearrangement can best be considered in terms of an intramolecular redox isomerization process. Further studies have shown the bridge to terminal rearrangement of the hydride ligand to be a significant step in cluster aggregation in the formation of $FePt_2$ and $FePt_3$ clusters.[7]

We are grateful to the Natural Science and Engineering Research Council of Canada for financial support of this work.

Received, 4th December 1986; Com. 1729

References

1 A. P. Humphries and H. D. Kaesz, *Prog. Inorg. Chem.*, 1979, **25**, 145.
2 A bridge–terminal–bridge rearrangement has been proposed to account for hydride scrambling in $H_4Ru(CO)_{10}(Ph_2PCH_2PPh_2)$: J. R. Shapley, S. I. Richter, M. R. Churchill, and R. A. Lashewycz, *J. Am. Chem. Soc.*, 1977, **99**, 7384.
3 P. M. Treichel, K. W. Dean, and W. M. Douglas, *Inorg. Chem.*, 1972, **11**, 1609.
4 F. G. A. Stone, *Inorg. Chim. Acta*, 1981, **50**, 33 and references therein.
5 J. Powell, J. F. Sawyer, and M. V. R. Stainer, *J. Chem. Soc., Chem. Commun.*, 1984, 1314.
6 M. Cygler, F. R. Ahmed, A. Forgues, and J. L. A. Roustan, *Inorg. Chem.*, 1983, **22**, 1026.
7 J. Powell, M. R. Gregg, and J. F. Sawyer, unpublished results.